Air Quality, Atmosphere & Health (2020) 13:259–269
https://doi.org/10.1007/s11869-020-00790-1

Solar radiation attenuation by aerosol: application to solar farms

Abdelmoula Ben-tayeb[1] · Mohammed Diouri[1] · Rajae Meziane[1] · Hanae Steli[1]

Received: 25 November 2019 / Accepted: 2 January 2020 / Published online: 9 January 2020

Abstract
The use of solar energy requires precise insolation knowledge of the considered site. Solar irradiance depends on geographical and astronomical parameters and variable characteristics of the atmosphere such as aerosol or cloud charge, which has a very important attenuation and pollution role. This study presents the estimate of the annual insolation of sites close to several solar farms. Insolation is calculated from Iqbal's basic formulas with introduction of the total optical thickness determined by the AERONET. The PSDs and aerosol loading on an atmospheric column allowed the establishment of the attenuation-aerosol concentration relationship. The cloudless atmosphere attenuates the incident solar flux by an annual average of the order of 23.5%, where in average, about 13.73% is attributed to the aerosol, 17.75% for solar farm sites near the Sahara, and 8% for California and Arizona US sites.

Keywords Aerosol optical thickness · Atmospheric aerosol · Insolation · Size distribution · Sun photometer · Solar farm

Introduction

Solar energy gains more importance as a source of renewable energy, creation of several solar farms, and personal use of solar water heaters. Expertise in choosing sites for solar farms requires knowledge of the annual atmospheric aerosol load. The efficiency of solar farms is more or less important depending on the attenuation produced in terms of incident solar radiation to the solar panels or to the receiving tower. This study is a specific contribution to the quantification of the attenuation by aerosols in solar farms.

Total solar radiation or the value of direct solar radiation outside the Earth varies over time due to solar radiation activity (Almorox and Hontoria 2004; Li et al. 2012); solar constant is its mean value. This solar constant is difficult to measure from the ground; the atmosphere attenuates a big part of the incoming electromagnetic waves. For this reason, the measuring stations were placed at high altitudes or suspended on balloons in the nineteenth century. Currently, the measuring instruments are placed on satellites, thereby giving a more precise value with a minimum of errors (Passos et al. 2007; Fröhlich 2009). Measurements of TSI were collected from 1976 to 2017 (Gueymard 2018). It appears that the daily change of the TSI within 42 years consists of 9 solar cycles of 11 years. In 2016, the value of 1361 W/m^2 was confirmed, which corresponds to the same value adopted by the International Astronomical Union (IAU 2015).

Depending on the latitude, the more you go north, the less solar irradiance becomes, earth's sphericity effect. The attenuation of solar irradiance by atmospheric components or by one of the elements of the atmosphere varies from one place to another according to the natural and anthropogenic charge of the atmosphere; an additional attenuation of 21.6% was observed in Mexico due to pollution (Jauregui and Luyando 1999), and it is directly related to the aerosol optical thickness (Frank et al. 2007; Zhang et al. 2012; Unsworth and Monteith 1972; Romano et al. 2013), which changes constantly according to the climatic conditions and the variability of the seasons (Kuzu and Saral 2017; Nam et al. 2018; Guleria and Kuniyal 2013; Nizar and Dodamani 2019). The atmospheric aerosol is one of the dominant factors in solar irradiance attenuation (Li et al. 1996). Many researchers have studied the effect of aerosols on solar irradiance (Hanrieder et al. 2015; Elias

✉ Abdelmoula Ben-tayeb
abdelmoulabentayeb@gmail.com

[1] Faculty of Science, Department of Physics, Team of Atmospheric Physic, Mohammed First University , Oujda, Morocco

et al. 2016). For example, the attenuation of solar radiation during a very dusty day reaches 40–50% in Greece because of desert dust (Kosmopoulos et al. 2017). Through the scattering and absorbing of solar radiation, aerosols change the physical properties of clouds, so the study of the physical and chemical properties of aerosols and their complex processes are important for climate prediction (Kuniyal and Guleria 2019). For all of the above, it was necessary to identify the influential components of the atmosphere (Tahiri et al. 2018; Diner et al. 2009; Meziane et al. 2019) and create prediction models for better use of solar irradiance due to its changing nature (Jimenez et al. 2016; Gueymard 2012).

The accumulation of dust on surface of panels in solar farms reduces their efficiency and thus lowers the energy extracted from the unit. This point has been the subject of several researches (Nipu et al. 2017; Ndiaye et al. 2013). The knowledge of aerosols properties, their volume distribution, and lifetime (Mahowald et al. 2014; Shuangshuang et al. 2019) allow the quantification of the layer of accumulated dust on solar panels. Experimental study of adhesion of air dust particles to the surface of solar panels in different climatic conditions was to remove particles by the airflow, in humid and in dry conditions (Du et al. 2019). The experimental results showed that the loss of efficiency of the solar panels gradually increased with the mass of accumulated dust, where 300 mg/m^2 accumulated for 1 week caused the loss of about 2.1% of efficiency (Jaszczur et al. 2019). The volume particle size distribution has already been studied and taken measurements at different locations and in different temperature conditions in southern Morocco (Diouri et al. 2009; Tahiri et al. 2016). Using the inversion approach (Hoyningen-Huene et al. 2009) to extract volume particle size distribution, a study was conducted in 2015 to understand the formation mechanisms of a dust layer in the free troposphere based on the (WRF-Chem) model and the collected dust observations (SAMUM-I) (Khan et al. 2015). Measurements taken in many cities suggest that fine particle concentrations are spatially more uniform than coarse particle ones (Wilson and Suh 1997). In an urban environment, the fine mode represents 60–70% of the aerosols, as the contribution of human to the pollution (Verma et al. 2014). In southern Italy, natural sources contributed on average 25.6% of fine particles and human sources about 74.4% (Trippetta et al. 2016).

The shortwave is used to produce more energy in photovoltaic cells, and the long wavelengths are used to produce less energy in thermal receptors. Photovoltaic cells have a good ability to absorb light from the visible spectrum to the near infrared spectrum. This absorption decreases with the increase of the wavelength and becomes very weak close to infrared (Lee et al. 2012; Yusoff et al. 2015). In a combined photovoltaic/thermal panel, the entire solar spectrum is used to produce electricity, and the residual heat is used for heating water.

Determining the insolation is limited to theoretical formulas similar to those of Iqbal, which do not take into account the atmospheric burden that can vary greatly between rural and urban areas in addition to the distance from the ocean. In this study, insolation was determined by inserting the total atmospheric optical thickness (TOT), knowing that in contrast to the gas molecules, aerosols interact with the entire continuous solar spectrum.

Sites and instrumentation

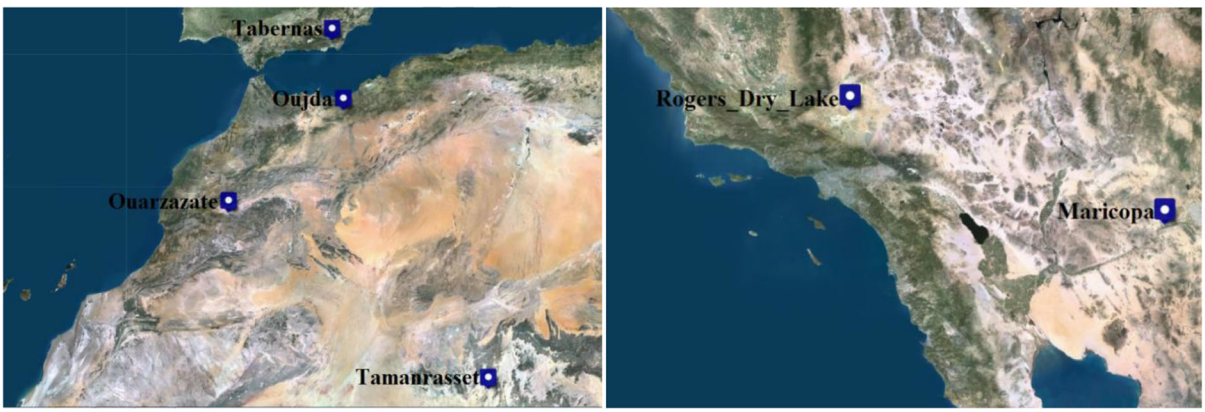

Station localizations

View of the sun photometer in Oujda (Morocco)

AERONET is a vast database containing the optical properties of aerosols from sites worldwide: measurements using CIMEL brand sun photometer with eight spectral channels (340, 380, 440, 500, 675, 870, 1020, and 1640 nm) based on remote sensing ground for the return of optical and microphysical properties of aerosols, vertically integrated on the atmospheric column, as well as other determinations such as size distribution, refractive index, and single scattering albedo (Holben et al. 2006). Used in this work, the optical thickness of the aerosols and the volume distribution of the particles of sites close to several solar farms (Table 1), these data are retrieved from almucantar scans of radiance at the same time with direct sunlight according to Dubovik and King (2000). Almucantar is a series of measurements taken at the elevation angle of the sun for specified azimuth angles relative to the position of the sun (Holben et al. 1998). The AOT uncertainties vary according to the wavelength of the solar radiation; in the visible and near infrared are estimated close ± 0.01 and in the UV at ± 0.02 (Holben et al. 1999; Eck et al. 1999).

Commonly, the used solar constant is measured by satellite and corresponding to the annual average 1367 W/m^2. The sun photometer measures the optical thickness corresponding to eight wavelengths, the corresponding solar spectrum constant is determined for each wavelength λ, taking into account the contribution of each λ to the total solar spectrum established by extraterrestrial solar spectral irradiance at mean sun-earth distance (Iqbal 1983).

Table 2 Example of relative I_0 (Wh) one day of each season

Site	I_0 1 July	I_0 1 October	I_0 1 January	I_0 1 April
Tabernas	11,558	7814	4338	9065
Rogers Dry Lake	11,525	8070	4711	9259
Oujda	11,520	8101	4758	9282
Maricopa	11,486	8280	5030	9414
Ouarzazate	11,432	8511	5394	9581
Tamanrasset	11,112	9279	6741	10,091

Solar irradiance

Solar irradiance expresses the amount of energy from the sun, received per unit area. If we do not take into account the attenuation by the atmosphere, their expression on horizontal surfaces is formulated for different time periods (Iqbal 1983). It depends on the eccentricity factor of the earth's orbit E_0, the geographic latitude ϕ, solar declination δ, the hour angle at the middle ω_i, and the solar constant I_{sc}; the solar irradiance on a horizontal plane over an hour is given by Eq. (1), and to calculate the solar irradiance for a period shorter than 1 hour, for example, between t_1 and t_2, we use Eq. (2):

$$I_0 = I_{SC}E_0(\sin\delta\sin\phi + (24/\pi)\sin(\pi/24)\cos\delta\cos\phi\cos\omega_i) \quad (1)$$

$$I_0\big|_{t_1}^{t_2} = I_{SC}E_0\{\sin\delta\sin(t_2-t_1) + (12/\pi)\cos\delta\cos\phi[\sin(15t_1)-\sin(15t_2)]\} \quad (2)$$

Table 2 shows examples of the solar irradiance without taking into account the atmosphere attenuation during a day of each season.

Table 1 Site characteristics (AERONET)

Site	Latitude	Longitude	Altitude (m)	Climate
Tabernas PSA-DLR (Spain)	37.09 N	2.35 W	500	Csa
Rogers Dry Lake (California)	34.92 N	117.88 W	680	Bsk
Oujda (Morocco)	34.65 N	1.89 W	620	Csa
Maricopa (Arizona)	33.06 N	111.97 E	360	Bwh
Ouarzazate (Morocco)	30.92 N	6.91 W	1136	Bwh
Tamanrasset_INM (Algeria)	22.79 N	5.53 E	1377	Bwh

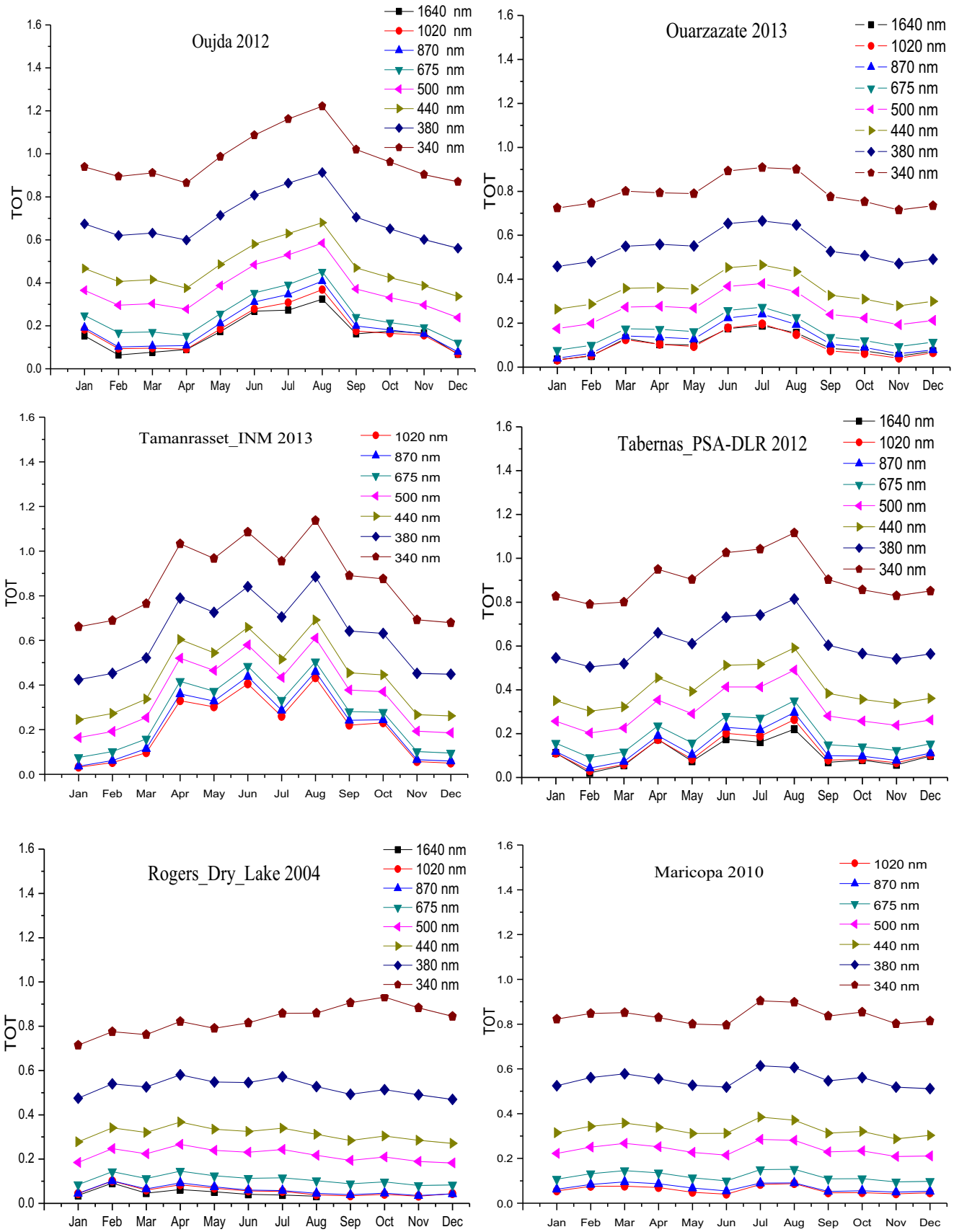

Fig. 1 Monthly average of TOT (λ)

Table 3 Annual averages of TOT and AOT for a shortwave 0.5 μm and a long wavelength 1.02 μm

Site	TOT		AOT	
	$SW_{0.5}$	$LW_{1.02}$	$SW_{0.5}$	$LW_{1.02}$
Ouarzazate 2013	0.262	0.097	0.109	0.071
Tamanrasset 2013	0.362	0.206	0.193	0.161
Tabernas 2012	0.304	0.117	0.129	0.076
Oujda 2012	0.329	0.135	0.184	0.124
Rogers Dry Lake 2004	0.218	0.053	0.069	0.038
Maricopa 2010	0.240	0.059	0.082	0.039

The value of I_0 depends on the number of the day and the latitude of the site. For determining the annual solar irradiation at a specific location, we integrate the solar irradiance regardless of the atmosphere I_0 during each hour from sunrise to sunset for every day of the year separately for each site. The calculated seasonal cycles are given for all the studied sites in the white hatched histograms (Fig. 2).

Effect of the atmosphere on solar irradiance

Optical thickness in cloudless atmosphere

Phenomena that contribute to the attenuation of solar radiation in cloudless atmosphere are the extinction due to aerosols, molecular diffusion (or Rayleigh), and gaseous absorption. Taking into account the relative air mass m_{air} cross by the solar radiation at every moment of day and the charge of the atmosphere by the insertion of the total atmospheric optical thickness TOT (λ), the attenuation of the irradiance is expressed with the Bouguer law on the wavelength λ by the following:

$$I(\lambda) = I_0(\lambda).\exp[-m_{\text{air}}.\text{TOT}(\lambda)] \quad (3)$$

TOT (λ) extracted from AERONET is the sum of the spectral contributions of Rayleigh interactions τ_{Ray}, τ_{aer} of aerosols, and gas τ_{gaz}.

$$\text{TOT}(\lambda) = \tau_{\text{Ray}}(\lambda) + \tau_{\text{aer}}(\lambda) + \tau_{\text{gaz}}(\lambda) \quad (4)$$

The relative air mass m_{air} expressed by Kasten and Young (1989) depends on the solar elevation, which was studied for Oujda site through characterization of different air mass influences in terms of aerosol optical parameters (El Amraoui and Diouri 2001). The daily average of the total spectral atmospheric thicknesses for all wavelengths is used to determine the effect of atmospheric components on the insolation of each site.

The methodology to find the solar irradiance attenuation made following three steps: (1) we have created and developed a program that calculates the solar irradiance without taking into account the atmosphere I_0 and the relative air mass for each moment of the day for a site by introducing their latitude. (2) Extract the total optical thicknesses of the atmosphere TOT and of aerosols AOT from AERONET and calculate the hourly average of TOT and AOT from sunrise to sunset during all the days of the year for all sites. (3) Insert the TOT and AOT data into the program to calculate the solar irradiance attenuation by the atmosphere (TE, total extinction) and by aerosols (AE, aerosol extinction).

In Fig. 1, we represent the monthly average variation of TOT at all used wavelengths and for all the studied sites.

The total atmospheric thickness for short wavelengths is larger than that of long wavelengths; for that, the attenuation of solar irradiance will be greater for ultraviolet radiation. Values less than 0.29 μm are totally eliminated from the stratosphere.

The monthly average atmospheric optical thickness at 0.5 μm for Maricopa and Rogers Dry Lake is almost stable throughout the year and respectively remains at around 0.2 and 0.1. For the other sites, TOT is high in summer and spring especially in August, in Oujda at 0.42 and in Tamanrasset at 0.6 because of the seasonal winds where the desert mineral dust is the predominant aerosol (Guirado et al. 2014). In Ouarzazate, the duration of the desert dust season differs from 1 year to another; consequently, the annual average aerosol optical thickness changes (Elias et al. 2016); the season of the dust in 2006 was the longest compared with 2012–2014 (Tesche et al. 2009).

For SW annual average, AOT is twice smaller than those of the TOT; the ratio is greater than three at US sites. For the LW, the deviations are quite low, on the order of 0.032 on average (Table 3).

Monthly irradiance

The fraction of attenuation of solar irradiance by atmospheric constituents excluding aerosols is almost of the order of 10% at all sites. Despite the long days in Tamanrasset, the presence of aerosol brings a great attenuation of the daily insolation; Fig. 2 shows that Tamanrasset receives a similar amount of solar seasonal radiation.

Atmospheric aerosols vary widely in concentration depending on geographic location, time, and altitude, as well as according to the characteristics of the source and seasonal changes depending on different weather characteristics and human activity. Low values of aerosol optical depth are observed in the high-altitude mountain station; AOT decreases with altitude (Alados-Arboledas et al.

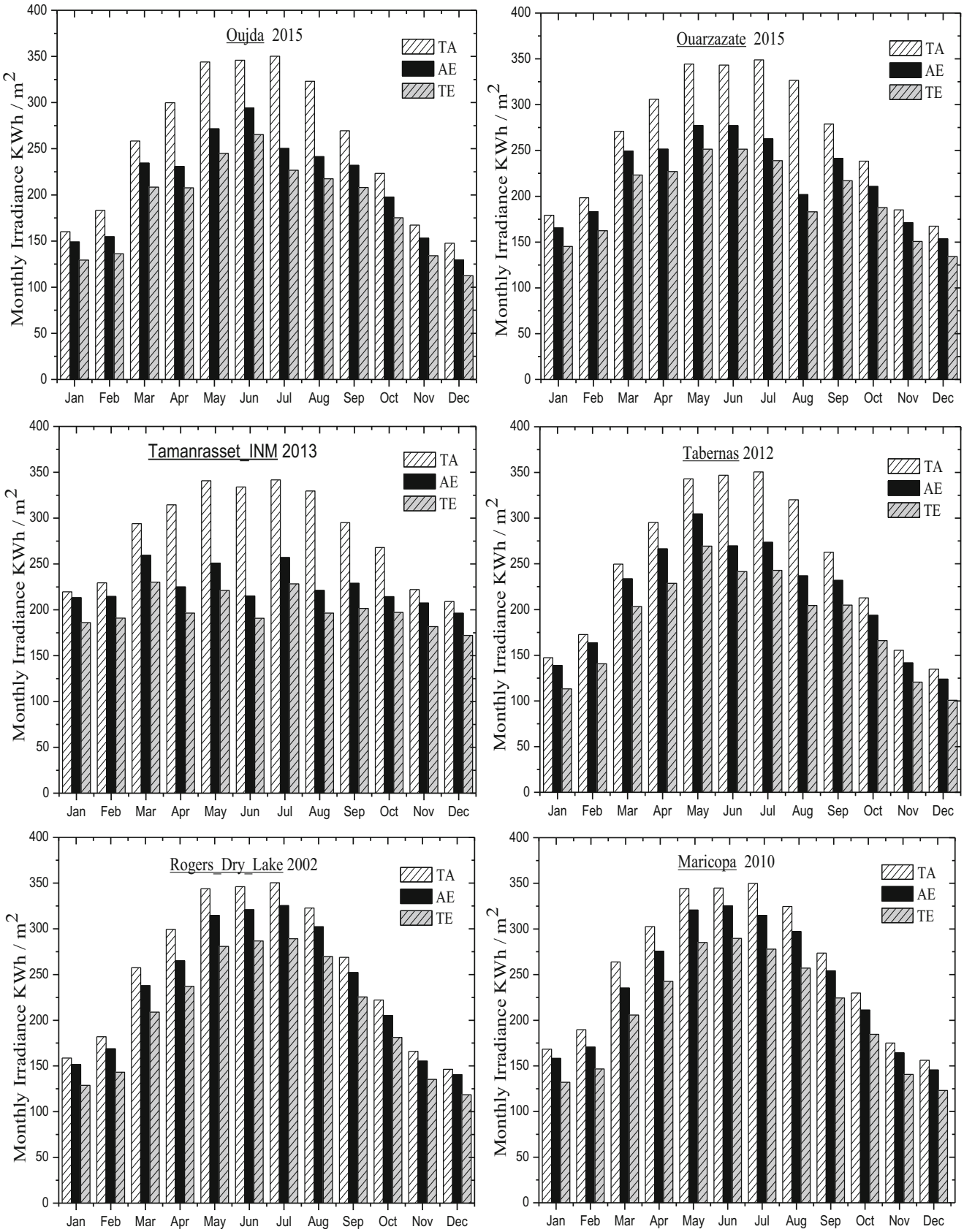

Fig. 2 Monthly variation of solar irradiance at top of atmosphere (TA), with aerosol extinction (AE), and with total extinction (TE)

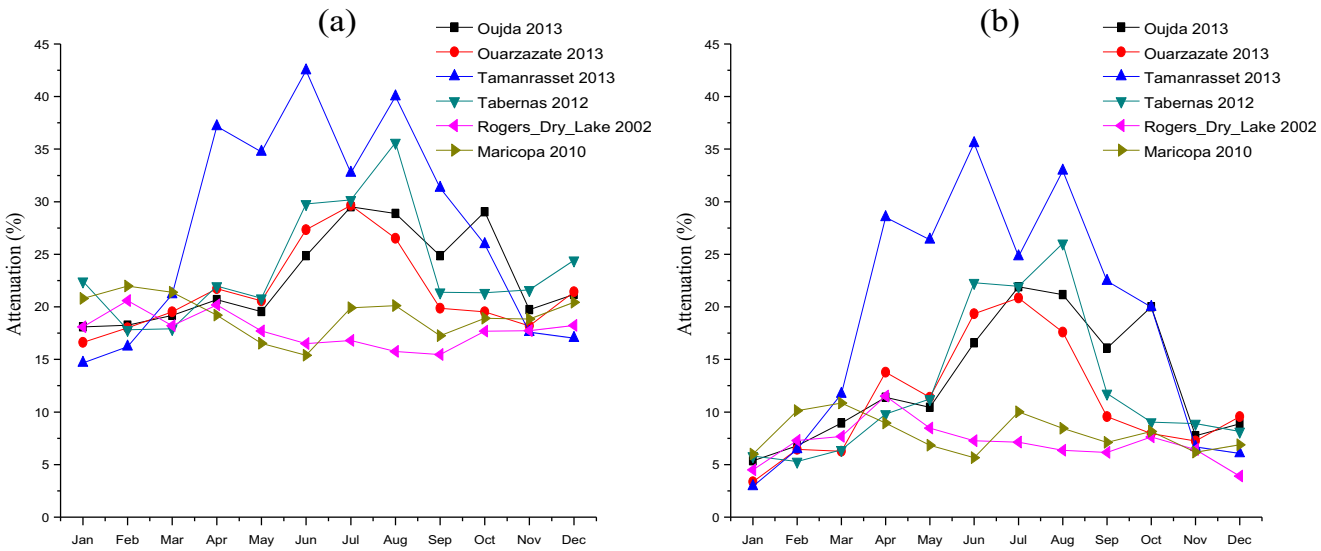

Fig. 3 Monthly average of attenuation fraction of solar irradiance by the atmosphere (**a**) and by aerosols (**b**)

2007). Aerosols are dominant in the troposphere and contribute significantly to the attenuation of the incident regional solar radiation.

Figure 3 shows the monthly average attenuation of solar irradiance by the atmosphere and by aerosols. There is a difference between the sites in terms of attenuation rate and the difference in attenuation between months at the same site. In Maricopa and Rogers Dry Lake, low annual atmospheric attenuation is around 18% with very low contribution of aerosol. For the other sites, important atmospheric attenuation especially from the beginning of spring until the middle of autumn with maximum 42.5% in June (Tamanrasset) and 35.6% in August (Tabernas) with very important contribution of the aerosol, Oujda also has a high attenuation 28% due to desert aerosols and aerosols due to human activities because it is a large urban center.

Table 4 shows the rate of solar irradiance attenuation by all the atmospheric components (TE) and by the atmospheric aerosols (AE) in Oujda and Ouarzazate during the period 2012–2015. There is a slight difference in attenuation rate of the same site from year to year, where the annual average of mitigation over the 4 years in Oujda (26.22 ± 2.79%) and Ouarzazate (24.60 ± 2.3%); the results confirm that aerosols are the dominant element of the atmosphere in terms of solar irradiance attenuation. The average annual aerosol attenuation over the 4 years in Oujda 17.23 ± 3.22% and Ouarzazate 15.59 ± 3.4% and the percentage of attenuation of solar irradiance by the other atmospheric constituents are almost of the order of 9 ± 1% for both sites.

Table 4 Annual average of attenuation of solar irradiance by the atmosphere (TE) and by the aerosols (AE) for the period 2012–2015

	Oujda		Ouarzazate	
	TE	AE	TE	AE
Average	0.26 ± 0.03	0.17 ± 0.03	0.24 ± 0.02	0.15 ± 0.03

Aerosol particle size distribution

The volume particle size distribution provides important information about aerosols and their effects on solar irradiance attenuation. The PSD is determined by inversion of the system of equations of the spectral optical thicknesses. Various studies and algorithms (Diouri and Sanda 1997; Diouri et al. 1997) have been developed, for the resolution of the inversion problem which determines the log normal distribution law of the number of particles per unit volume representing the aerosol population, and from which, we deduce the volume distributions shown in Fig. 4, Table 5.

Figure 4 illustrates monthly average of the aerosol particle size distribution. These determinations confirm the existence of two volume size modes, the fine around 0.13 μm with small amplitude. The coarse mode is the dominant with median radius of near 2.8 μm.

Atmospheric aerosols have extremely variable concentrations depending on the geographic area and altitude; the volume distribution of aerosols for the coarse mode in the sites near the Sahara (Ouarzazate, Tamanrasset, Oujda) is very high during the dry season from May to September, with maximum 0.32 $\mu m^3/\mu m^2$ in Tamanrasset during June, Oujda 0.22 $\mu m^3/\mu m^2$, and Ouarzazat 0.11 $\mu m^3/\mu m^2$ during August, due to the impact caused by the desert storm advections that characterize this period. In Tabernas, there is a significant increase in the volume distribution of aerosols for the coarse mode in April

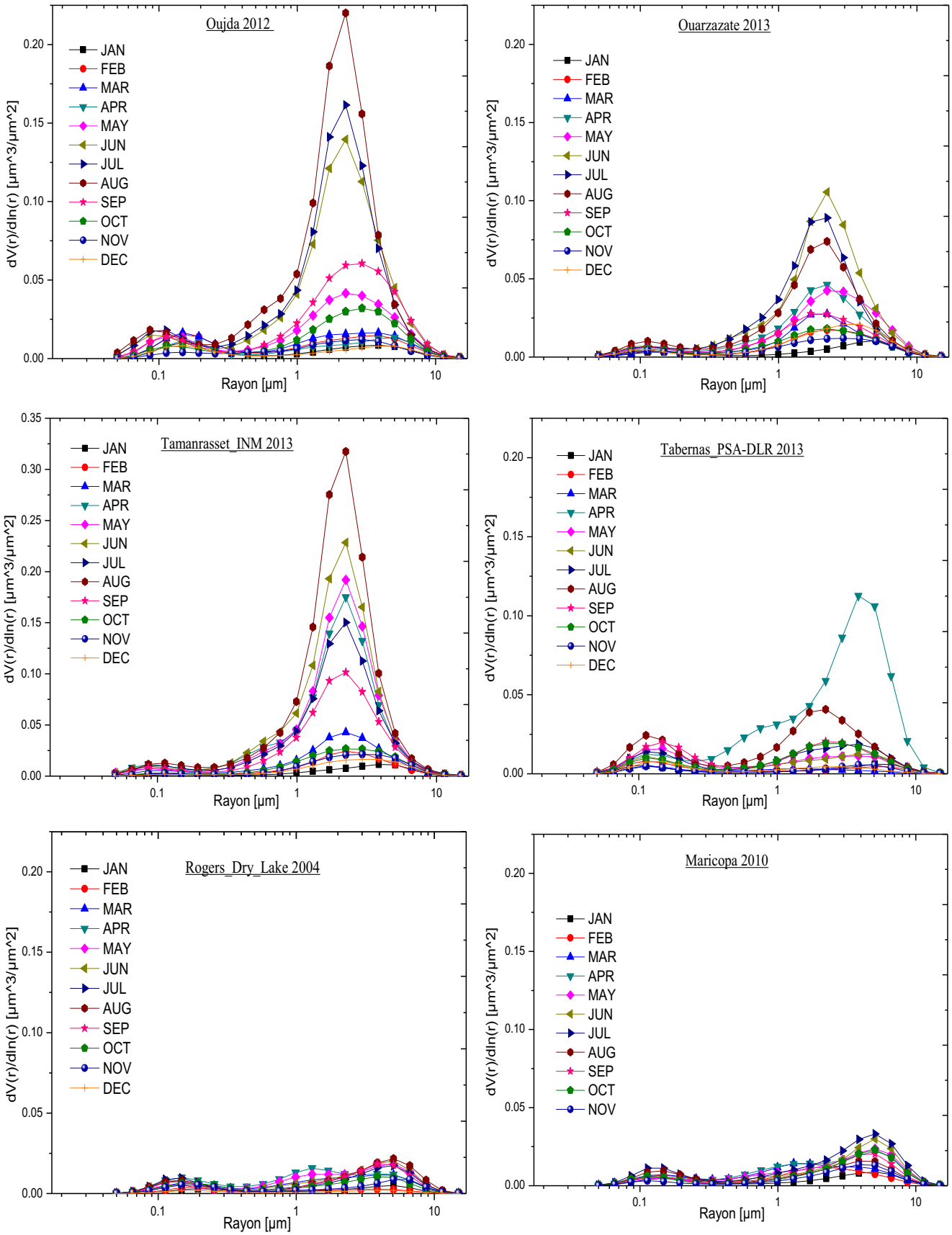

Fig. 4 Monthly average of aerosol particle size distributions

Table 5 Annual mean of particle size distribution parameters, fine and coarse median radius r_f and r_c (μm), fine and coarse volume concentrations V_f and V_c, and total volume concentrations V_t ($\mu m^3/\mu m^2$)

Site	Fine mode		Coarse mode		V_t
	r_f	V_f	r_c	V_c	
Ouarzazate	0.11	0.008	2.62	0.061	0.069
Tamanrasset INM	0.10	0.011	2.49	0.134	0.145
Tabernas PSA-DLR	0.12	0.013	4.62	0.035	0.048
Oujda	0.12	0.016	3.18	0.084	0.1
Rogers Dry Lake	0.16	0.007	4.45	0.020	0.027
Maricopa	0.13	0.008	4.24	0.031	0.039

Table 6 Annual mean of aerosol volume particle size distribution parameters for the period 2012–2015 for Ouarzazate and Oujda. Fine and coarse median radius r_f and r_c (μm) and fine and coarse volume concentrations V_f and V_c ($\mu m^3/\mu m^2$)

Site	r_f	V_f	r_c	V_c
Oujda	0.14 ± 0.02	0.015 ± 0.001	2.72 ± 0.46	0.075 ± 0.016
Ouarzazate	0.14 ± 0.03	0.010 ± 0.002	2.55 ± 0.13	0.082 ± 0.021

0.11 $\mu m^3/\mu m^2$. Maricopa and Rogers Dry Lake sites register similar low concentrations of fine and coarse particles not exceeding 0.031 $\mu m^3/\mu m^2$. Low irregularity of aerosol parameters was registered during the period 2012–2015 for Oujda and Ouarzazate (Table 6).

Figure 5 shows the linear fit of attenuation which represents attenuation of solar irradiance by the atmosphere (a) and by aerosols (b). Through this representation, attenuation can be determined according to volume concentrations by an affine function. The total volume concentration is practically equivalent to that of the coarse particles.

Conclusion

Solar energy acquires a renewed interest growing among renewable energy. There is a need to know accurately the intensity of solar radiation on the Earth surface for the use of solar energy. The study of constraints, particularly those related to aerosol atmospheric loading, makes it possible to estimate the dust accumulated on solar panels or solar park mirrors that block a large part of the radiation and reduce their energy efficiency. The study of the optical properties of the atmospheric aerosol enables accurate determination of the attenuation of solar radiation that can be observed at any time.

The sites close to the Sahara, the first major desert dust reservoir, are characterized by a high concentration of coarse particles in the atmosphere; the stations closest to the Sahara should receive more particles and therefore require considerable additional effort to clean the panels, photovoltaic, and solar mirrors.

The determined PSDs observed a mean fine mode of 0.12 ± 0.04 μm with low amplitude and a mean coarse mode of 3.6 ± 0.85 μm with amplitude eight times higher for sites near the Sahara. This ratio drops to four for the US sites, so they have less energy efficiency losses due to the low aerosol load.

The cloudless atmosphere attenuates annual average 23.5% of the incident solar energy flux which 17.75% is attributed to the attenuation by aerosols for sites near the Sahara. This percentage drops to 8% for US sites. This attenuation due to atmospheric aerosol observes a linear variation as a function of the volume concentration of the particles with a slope of the order of 1.12 and a main contribution of the coarse particle mode.

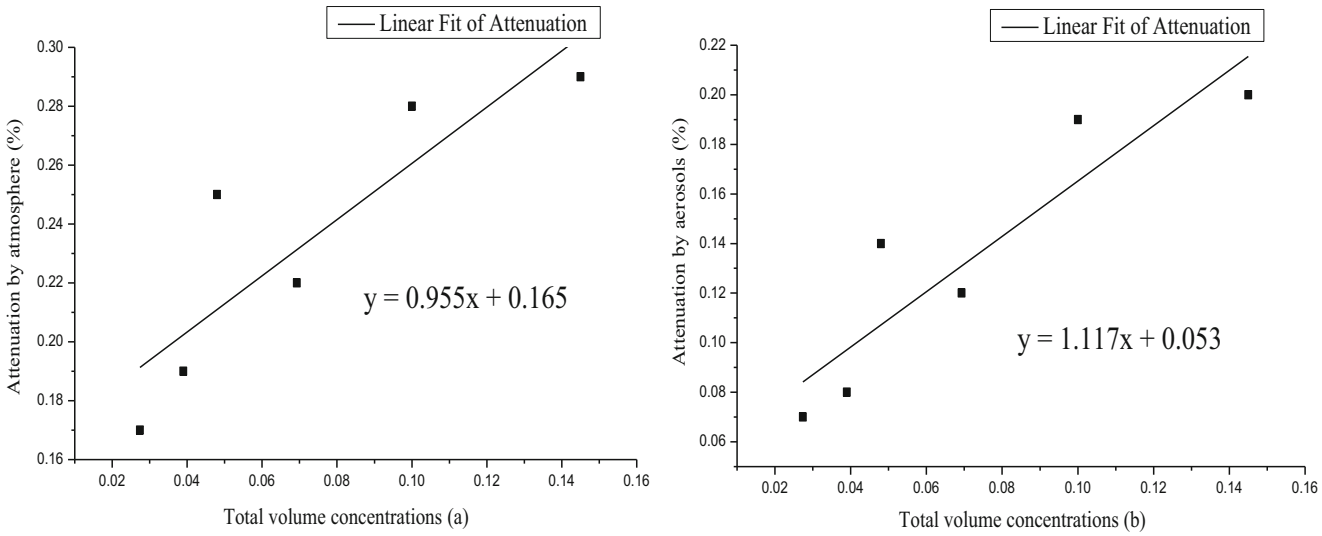

Fig. 5 Attenuation by the atmosphere (**a**) and by aerosols (**b**) according to the total volume concentration

Acknowledgments The authors want to thank AERONET's IPs: Stefan Wilbert, Emilio Cuevas-Agullo, Brent Holben, and Jeannette van den Bosch.

References

Alados-Arboledas L, Rascado JLG, Lyamani H, Navas-Guzmán F, FJO R (2007) Characterization of the atmospheric aerosol by combination of LIDAR and sun-photometry. Proc SPIE 6750:67500J–675001J. https://doi.org/10.1117/12.737557

Almorox J, Hontoria C (2004) Global solar radiation estimation using sunshine duration in Spain. Energy Convers Manag 45:1529–1535

Diner T, Hoyningen-Huene WV, Burrows JP, Kokhanovsky A, Bierwirth E, Wendisch M, Muller D, Kahn R, Diouri M (2009) Retrieval of aerosol optical thickness for desert conditions using MERIS observations during the SAMUM campaign. Tellus 61B:229–238

Diouri M, Sanda IS (1997) Deduction of particle size distribution from aerosol optical depth CLEOPATRE I code. J Aerosol Sci 28(p):459

Diouri M, El Hitmy M, Sanda IS, Jaenicke R, Kulzer S, Leiterer U, Schutz L, Schultz KH (1997) Indirect determination of particle size distribution using a sunphotometer at Lidenberg (Germany) and Oujda (Morocco). J Aerosol Sci 28(p):401

Diouri M, Hoyningen-Huene WV, Zarrouk T, Dinter T, Kokhanovsky A, Burrows JP (2009) Determination of aerosol particle size distribution for mineral dust during the SAMUM campaign. European Aerosol Conference, Karlsruhe Abstract T052A16

Du X, Jiang F, Liu E, Wu C, Ghorbel FH (2019) Turbulent airflow dust particle removal from solar panel surface: analysis and experiment. J Aerosol Sci 130(2019):32–44

Dubovik O, King MD (2000) A flexible inversion algorithm for retrieval of aerosol optical properties from sun and sky radiance measurements. J Geophys Res 105:20,673–20,696

Eck TF, Holben BN, Reid JS, Dubovik O, Smirnov A, O'Neill NT, Slutske I, Kinne S (1999) Wavelength dependence of the optical depth of biomass burning, urban, and desert dust aerosols. J Geophys Res 104(D24):31333–31349. https://doi.org/10.1029/1999JD900923

El Amraoui L, Diouri M (2001) Characterisation of different air mass influences in terms of aerosol optical parameters. J Aerosol Sci 32(Supp1):S643–S644

Elias T, Ramon D, Dubus L, Bourdil C, Cuevas-Agulló E, Zaidouni T, Formenti P (2016) Aerosols attenuating the solar radiation collected by solar tower plants: the horizontal pathway at surface level. AIP Conf Proc 1734:150004. https://doi.org/10.1063/1.4949236

Frank TD, Girolamo LD, Geegan S (2007) The spatial and temporal variability of aerosol optical depths in the Mojave Desert of southern California. Remote Sens Environ 107:54–64

Fröhlich C (2009) Evidence of a long-term trend in total solar irradiance. Astron Astrophys 501:L27–L30. https://doi.org/10.1051/0004-6361/200912318

Gueymard CA (2012) Temporal variability in direct and global irradiance at various time scales as affected by aerosols. Sol Energy 86:3544–3553

Gueymard CA (2018) A reevaluation of the solar constant based on a 42-year total solar irradiance time series and a reconciliation of spaceborne observations. Sol Energy 168(2018):2–9

Guirado C, Cuevas E, Cachorro VE, Toledano C, Alonso-Pérez S, Bustos JJ, Basart S, Romero PM, Camino C, Mimouni M, Zeudmi L, Goloub P, Baldasano JM, de Frutos AM (2014) Aerosol characterization at the Saharan AERONET site Tamanrasset. Atmos Chem Phys 14:11753–11773

Guleria RP, Kuniyal JC (2013) Aerosol climatology in the northwestern Indian Himalaya: a study based on the radiative properties of aerosol. Air Qual Atmos Health 6:717–724. https://doi.org/10.1007/s11869-013-0206-y

Hanrieder N, Wilbert S, Pitz-Paal R, Emde C, Gasteiger J, Mayer B, Polo J (2015) Atmospheric extinction in solar tower plants: absorption and broadband correction for MOR measurements. Atmos Meas Tech 8:3467–3480

Holben BN, Eck TF, Slutsker I, Tanre D, Buis JP, Setzer A, Vermote E, Reagan JA, Kaufman YJ, Nakajima T, Lavenu F, Jankowiak I, Smirnov A (1998) AERONET—a federated instrument network and data archive for aerosol characterization. Remote Sens Environ 66:1–16

Holben BN, Tanré D, Smirnov A, Eck TF, Slutsker I, Dubovik O, Lavenu F, Abuhassen N, Chatenet B (1999) Optical properties of aerosol from long term ground-based AERONET measurements. In: Proc. ALPS99, 17-23 January 1999, Meribel, France, WK1-O-19. https://scholar.google.com/scholar_lookup?title=Optical%20properties%20of%20aerosols%20from%20long%20term%20groundbased%20aeronet%20measurements&publication_year=1999&author=Holben%2CBN&author=Tanr%C3%A9%2CD&author=Smirnov%2CA&author=Eck%2CTF&author=Slutsker%2CI&author=Dubovik%2CO&author=Lavenu%2CF&author=Abuhassen%2CN&author=Chatenet%2CB

Holben BN, Eck TF, Slutsker I, Smirnov A, Sinyuk A, Schafer J, Giles D, Dubovik O (2006) Aeronet's Version 2.0 quality assurance criteria. In: SPIE Asia-Pacific Remote Sensing, 2006, Goa, India. Proceedings Volume 6408, Remote Sensing of the Atmosphere and Clouds; 64080Q. https://doi.org/10.1117/12.706524

Hoyningen-Huene WV, Dinter T, Kokhanovsky AA, Burrows JP, Wendisch M, Bierwirth E, Muller D, Diouri M (2009) Measurements of desert dust optical characteristics at Porte au Sahara during SAMUM. Tellus 61B:206–215

IAU (2015) Resolution B3 on Recommended Nominal Conversion Constants for Selected Solar and Planetary Properties. https://arxiv.org/abs/1510.07674v1. Accessed 13 Aug 2015

Iqbal M (1983) An introduction to solar radiation. Academic Press, Toronto

Jaszczur M, Teneta J, Styszko K, Hassan Q, Burzyńska P, Marcinek E, Łopian N (2019) The field experiments and model of the natural dust deposition effects on photovoltaic module efficiency. Environ Sci Pollut Res 26:8402–8417. https://doi.org/10.1007/s11356-018-1970-x

Jauregui E, Luyando E (1999) Global radiation attenuation by air pollution and its effects on the thermal climate in Mexico City. Int J Climatol 19:683–694

Jimenez PA, Hacker JP, Dudhia J, Haupt SE, Ruiz-Arias JA, Gueymard CA, Thompson G, Eidhammer T, Deng A (2016) WRF-solar: description and clear-sky assessment of an augmented NWP model for solar power prediction. Bull Am Meteorol Soc 97:1249–1264. https://doi.org/10.1175/BAMS-D-14-00279.1

Kasten F, Young AT (1989) Revised optical air mass and approximation formula. Appl Opt 28:4735–4738

Khan B, Stenchikov G, Weinzierl B, Kalenderski S, Osipov S (2015) Dust plume formation in the free troposphere and aerosol size distribution during the Saharan mineral dust experiment in North Africa. Tellus B 2015(67):27170

Kosmopoulos PG, Kazadzis S, Taylor M, Athanasopoulou E, Speyer O, Raptis PI, Marinou E, Proestakis E, Solomos S, Gerasopoulos E, Amiridis V, Bais A, Kontoes C (2017) Dust impact on surface solar irradiance assessed with model simulations, satellite observations and ground-based measurements. Atmos Meas Tech 10:2435–2453

Kuniyal JC, Guleria RP (2019) The current state of aerosol-radiation interactions: a mini review. J Aerosol Sci 130:45–54

Kuzu SL, Saral A (2017) The effect of meteorological conditions on aerosol size distribution in Istanbul. Air Qual Atmos Health 10:1029–1038. https://doi.org/10.1007/s11869-017-0491-y

Lee MM, Teuscher J, Miyasaka T, Murakamian TN, Snaith HJ (2012) Efficient hybrid solar cells based on meso-superstructured organometal halide perovskites. Science 338(6107):643–647

Li X, Maring H, Savoie D, Voss K, Prospero JM (1996) Dominance of mineral dust in aerosol light-scattering in the North Atlantic trade winds. Nature 380:416–419

Li KJ, Feng W, Xu JC, Gao PX, Yang LH, Liang HF, Zhan LS (2012) Why is the solar constant not a constant? Astrophys J 747:135. https://doi.org/10.1088/0004-637X/747/2/135

Mahowald N, Albani S, Kok JF, Engelstaeder S, Scanza R, Ward DS, Flanner MG (2014) The size distribution of desert dust aerosols and its impact on the Earth system. Aeolian Res 15:53–71

Meziane R, Diouri M, Ben-tayeb A (2019) Optical aerosol properties of megacities: inland and coastal cities comparison. Air Qual Atmos Health:1–9. https://doi.org/10.1007/s11869-019-00769-7

Nam J, Kim SW, Park RJ, Park JS, Park SS (2018) Changes in column aerosol optical depth and ground-level particulate matter concentration over East Asia. Air Qual Atmos Health 11:49–60. https://doi.org/10.1007/s11869-017-0517-5

Ndiaye A, Kébé CMF, Ndiaye PA, Charki A, Kobi A, Sambou V (2013) Impact of dust on the photovoltaic (PV) modules characteristics after an exposition year in Sahelian environment: the case of Senegal. Int J Phys Sci 8(21):1166–1173. https://doi.org/10.5897/IJPS2013.3921

Nipu NN, Saha A, Khan MF (2017) Effect of accumulated dust on the performance of solar PV module. Int J Eng Technol 6(1):9–12

Nizar S, Dodamani BM (2019) Spatiotemporal distribution of aerosols over the Indian subcontinent and its dependence on prevailing meteorological conditions. Air Qual Atmos Health 12:503–517. https://doi.org/10.1007/s11869-019-00677-w

Passos D, Brandao S, Lopes I (2007) On the luminosity evolution of the sun during the last 7 millennia. Adv Space Res 40:990–995

Romano F, Ricciardelli E, Cimini D, Paola FD, Viggiano M (2013) Dust detection and optical depth retrieval using MSG-SEVIRI data. Atmosphere 4:35–47

Shuangshuang S, Honglei W, Bin Z, Zhendong G (2019) Characterization of aerosol size distributions and chemical compositions under strong wind and stagnant conditions during haze episodes in Lin'an, China. Air Qual Atmos Health 12:1469–1481. https://doi.org/10.1007/s11869-019-00752-2

Tahiri A, Diouri M, Steli H, Marsli I, Meziane R, Ben-tayeb A (2016) Desert aerosol optical properties in Morocco. Environ Sci Hikari Ltd 4:63–78. https://doi.org/10.12988/es.2016.631

Tahiri A, Diouri M, Barkani J (2018) Optical properties of desert aerosol-I. J Mater Environ Sci 9(10):2870–2883

Tesche M, Ansmann A, Müller D, Althausen D, Mattis I, Heese B, Freudenthaler V, Wiegner M, Esselborn M, Pisani G, Knippertz P (2009) Vertical profiling of Saharan dust with Raman lidars and airborne HSRL in southern Morocco during SAMUM. Tellus 61B:144–164

Trippetta S, Sabia S, Caggiano R (2016) Fine aerosol particles (PM1): natural and anthropogenic contributions and health risk assessment. Air Qual Atmos Health 9:621–629. https://doi.org/10.1007/s11869-015-0373-0

Unsworth MH, Monteith JL (1972) Aerosol and solar radiation in Britain. Q J R Meteorol Soc 98:778–797. https://doi.org/10.1002/qj.49709841806

Verma S, Bhanja SN, Pani SK, Misra A (2014) Aerosol optical and physical properties during winter monsoon pollution transport in an urban environment. Environ Sci Pollut Res 21:4977–4994. https://doi.org/10.1007/s11356-013-2383-5

Wilson WE, Suh HH (1997) Fine particles and coarse particles: concentration relationships relevant to epidemiologic studies. J Air Waste Manage Assoc 47:1238–1249

Yusoff ARM, Kim D, Schneider FK, da Silva WJ, Jang J (2015) Au-doped single layer graphene nanoribbons for a record-high efficiency ITO-free tandem polymer solar cells. Energy Environ Sci 8:1523–1537

Zhang Y, Yu H, Eck TF, Smirnov A, Chin M, Remer LA, Bian H, Tan Q, Levy R, Holben BN, Piazzolla S (2012) Aerosol daytime variations over North and South America derived from multiyear AERONET measurements. J Geophys Res 117:D05211